Optical Polarimetry and Mechanical Rheometry of Poly(ethylene oxide)−Silica Dispersions

Qiang Zhang and Lynden A. Archer*

School of Chemical and Biomolecular Engineering, Cornell University, Ithaca, New York 14853

Received November 6, 2003; Revised Manuscript Received December 28, 2003

ABSTRACT: Mesoscale structural dynamics and rheology of semidilute aqueous dispersions of poly(ethylene oxide) (PEO) containing nanosized silica particles are investigated using mechanical rheometry, optical polarimetry, and dynamic light scattering measurements. The average diameter of silica particles in the dispersions is chosen to be much smaller than the polymer coil diameter to study the effect of polymer−particle interactions on solution properties. For particle volume fractions as low as 0.2%, a nearly 2-fold increase in the solution viscosity and optical anisotropy is observed. At a particle volume fraction of 2% the viscosity and optical birefringence are an order of magnitude larger than in the neat polymer solutions. At low shear rates, polymer−nanoparticle dispersions manifest larger stress−optical ratios than the neat polymer solutions; they violate the stress−optical rule at high shear rates. Nanoparticles are also found to dramatically slow down stress relaxation of the solutions and to shift the onset of shear thinning behavior to lower shear rates. These findings are discussed in terms of the polymer bridging effect, which produces soft colloidal structures that are larger in size than either the polymer or primary particles. Slower dynamics of these secondary structures and flow-induced changes of their shape are argued to produce other properties observed.

Introduction

Polymer−particle dispersions find applications in a growing number of products, including paints and coatings, inks, cosmetics, and pharmaceutical formulations, and recently in synthesis of nanocomposite materials.[1,2] Flow behavior of dispersions is very important in all of these applications[3] and therefore worthy of in-depth study. The common case is that small amounts of water-soluble polymers are used as flocculants for unwanted particulate material in water or as stabilizers for particle suspensions such as in paints.[4,5] In this study, the opposite case is considered. A small amount of true nanosized particles is added to polymer solutions and their effect on flow properties studied in detail. If the average diameter of primary particles is comparable to the coil size of polymer molecules, interesting non-continuum effects similar to those observed in nanocomposite materials[6−8] are expected to emerge, providing novel strategies for controlling flow properties of polymeric fluids. Specifically, when nanoparticles strongly adsorb the surrounding polymer chains, the polymer ceases to provide a continuum medium for particle support. Individual polymer chains can physically adsorb to multiple particles[9] even at very modest particle loadings, resulting in a strong bridging effect and spontaneous formation of deformable colloidal structures in the dispersion.

Fluid flow properties of polymer−nanoparticle dispersions are very sensitive to the presence of deformable polymer−particle superstructures.[4−6,10] Horigome and Otsubo for example studied aqueous suspensions of polystyrene beads (average diameter $\bar{d}$ = 124 nm, particle volume fraction ϕ = 30%) flocculated by polymers ($\overline{M_w}$ = 25 000 g/mol) with associating end functional groups.[5] These end groups can associate with particle surface as well as with each other. Dynamic rheological properties of the suspensions were found to remain highly elastic even at low deformation frequencies. These authors contend that this behavior is related to formation of secondary structures where particles are bridged by associating polymer chains. In steady shear experiments, these suspensions exhibit Newtonian behavior at extremely low shear rate (of the order of 10^{-5} s^{-1}), suggesting polymer bridges are constantly breaking and re-forming in a quiescent state.

When the particle size is reduced from microns or submicrons to nanometers, a much lower particle volume fraction is required to form percolated polymer−particle superstructures. Zhang and Archer[6] recently studied the viscoelastic properties of various model poly(ethylene oxide) (PEO)−silica nanocomposites at temperatures above the melting point of PEO. These authors observed that spherical silica particles ($\bar{d}$ = 12 nm) dispersed in narrow molecular weight distribution PEO (average random coil diameter $d_{PEO} \sim$ 20 nm) melts dramatically increase the stress relaxation time (by more than 3 orders of magnitude, compared to the neat polymer) at particle volume fractions as low as 2%. These observations are particularly interesting because the threshold required for randomly dispersed hard spheres to form a percolated network is nearly 15 times the particle concentration where the strong retardation of fluid relaxation is observed. This indicates that bare particle−particle jamming contacts are not likely the source of slowing down of stress relaxation. The authors instead attributed their observations to the presence of soft, deformable colloids spontaneously formed in the system by polymer bridging interactions. The adsorption of PEO onto silica particles is widely believed to be irreversible due to hydrogen bonding.[11] Such soft polymer−particle clusters can be shown to produce a percolated network that is the source of their experimental observations.

Microstructure and flow-induced structural changes of polymer−particle dispersions are more complicated compared with those of pure polymer solutions. Although polymer−particle clusters are known to play important roles in flow properties of these dispersions,

10.1021/ma035667v CCC: $27.50
Published on Web 02/07/2004

understanding of their flow dynamics remains less thorough and quantitative than pure polymer solution dynamics. While it is in principle possible to estimate the size of the polymer−particle clusters and their effect on fluid relaxation time in a continuum model by describing the bridging effect as an extra attractive interaction between particle surfaces,[12] the strength of this attraction requires detailed knowledge of the chain structure in the bridges[13,14] and the adsorption characteristics of polymer chains onto colloidal particles.[15] In the case of planar surfaces, these effects are known and the interactions can be modeled using scaling approaches (see, for example, de Gennes[13] and Scheutjens and Fleer[14]) or computer simulations.[16] When the particle diameter becomes comparable to or even smaller than the equilibrium polymer coil size, however, the particle curvature cannot be ignored. This introduces new complications that must be resolved for quantities such as the average cluster size, number of particles per cluster, and equilibrium polymer configurations between particles in a cluster to be determined.

Optical polarimetry has become an important experimental approach for studying flow properties of colloidal dispersions and other complex fluids.[10,17] Schmidt et al.[10] investigated rheology and flow birefringence of PEO−clay aqueous dispersions. PEO and clay platelets have flow birefringence with opposite signs. Elastic behavior at low oscillatory frequencies and yield phenomenon observed in rheology experiments suggest the existence of a polymer−clay network in which a dynamic adsorption/desorption equilibrium is held. Results of birefringence measurement indicated that clay platelets were easily oriented at low shear rates. Polymer chains started to stretch above a critical shear rate and their contribution of flow birefringence becomes dominant at high shear rates. However, because of the strong birefringence of both components, these authors could not separate their individual contributions and hence could not extract more quantitative information on relaxation dynamics of each component.

In this study we use multiple experimental tools (mechanical rheometry, optical polarimetry, and dynamic light scattering) to determine how the mesoscopic structure of polymer−nanoparticle dispersions influences their stress relaxation behavior. PEO−silica aqueous dispersions with polymer and particle characteristics similar to those used in the earlier study[6] are the model system of this work. The presence of water in the current systems is not expected to significantly weaken the strong polymer adsorption onto particles.[11] Mesoscale clusters similar to those argued to exist in the melt are therefore anticipated in the dispersions. At the same time, the polymer concentration is high enough to avoid flocculation due to direct particle−particle contacts. By combining mechanical rheometry and optical birefringence measurements, the contribution of these clusters to the overall flow response is more easily isolated from the polymer solution background.

Experiment

Materials. Two linear PEOs with narrow molecular weight distribution and with the following molecular structure $CH_3O-[CH_2CH_2O]_n-H$ were purchased from Polymer Source, Inc. One polymer has $\overline{M}_w$ of 700 000 g/mol ($\overline{M}_w/\overline{M}_n = 1.06$) and the other $\overline{M}_w$ of 178 000 g/mol ($\overline{M}_w/\overline{M}_n = 1.09$). Narrow size distribution silica particles with $d = 12$ nm and specific surface area of 220 m^2/g (Ludox AS30 Colloidal Silica from Sigma Aldrich, Inc.) and $d = 100$ nm (Polyscience, Inc.) were used in the study. Surface-modified silica particles were created by tethering the particle surface with 2-[methoxy(polyethyleneoxy)propyl]trimethoxysilane, $(CH_3(CH_2CH_2O)_{6-9}(CH_2)_3Si(OCH_3)_3$ (from Gelest, Inc.)). For simplicity, we use the nomenclature o-PEO silane to identify this material in the following sections. According to the manufacturer, the specific wetting surface of o-PEO silane (the minimum amount of silane required to provide a uniform surface layer) is around 150 m^2/g.

PEO−silica aqueous dispersions were prepared using the following procedure. First, PEO was dissolved in deionized water to produce a 10 wt % aqueous solution. The aqueous silica suspension purchased from the manufacturer was also diluted with deionized water. If surface coated silica particles were to be used, o-PEO silane was added to the suspension. To ensure high surface coverage, excess o-PEO silane was used so that its total wetting surface area was around 5% larger than the total surface area of silica particles. Next, the diluted silica suspension was dispersed into an aqueous PEO solution. The mixture was diluted to the desired concentration and shaken for about 2 weeks in order for homogeneous dispersion of particles. Most samples prepared in this way contain a small amount of ions (usually the ion concentration is of the order of 0.01 mol %) that comes from electrostatically stabilized colloidal silica suspensions.

Homogeneity of polymer chains in PEO−silica dispersions is important. The polymer concentration in these dispersions ranges from 0 to 4.6 wt %. At these concentrations, neat PEO solutions are clear and transparent. In addition, their linear rheology shows a clear transition to terminal behavior at oscillation frequencies below λ^{-1}, where λ is the terminal molecular relaxation time. These facts confirm that PEO chains are completely dissolved and the solutions are homogeneous.

These dispersions are also quite stable. Their dynamic properties have been observed to remain unchanged for more than half a year, and all experimental results shown in this article are repeatable with the same sample. This is because the polymer concentration is high enough to maintain strong steric repulsions between particles, which efficiently stabilize particles at their secondary minimum.

Optical Polarimetry. Optical polarimetry was used to measure the flow birefringence of PEO solutions and PEO−silica dispersions. The experimental setup is from a previous study[17] with slight modifications. The sample was placed in the Couette flow cell shown in Figure 1, and all measurements were performed at room temperature. This cell has an inner stationary bob and a rotating cylinder that generates simple shear flow. The stationary bob is attached to a moving stage that adjusts the bob position relative to the cylinder. The cylinder was connected with a variable step motor via a timing belt. The diameter of the bob is 23.25 mm, and the gap between the bob and the cylinder is 1.25 mm. As the gap is much smaller than the bob diameter, curvature effects are minimized. The optical path length d is 25.4 mm. Using this arrangement, shear rates between 10^{-3} and 10^3 s^{-1} can be generated.

Figure 1 also shows a sketch of the optical train. Monochromatic light in the $-z$ direction is generated by a He−Ne laser source (wavelength $\lambda = 632.8$ nm) and consecutively passes through a polarizer (P), a photoelastic modulator (PEM), a quarter-wave plate (QWP), the flow cell, and a circular polarizer (CP) and received by a GaAs photodetecter. The time-dependent signal measured by the photodetecter can be written in the form of Fourier series up to the third term:

$$I(t) = \frac{I_0}{2}[1 - 2J_1(A)\cos(2\chi)\sin\delta'\sin(\omega t) - 2J_2(A)\sin(2\chi)\sin\delta'\cos(2\omega t)] + \ldots \quad (1)$$

Here, A is the amplitude of the oscillatory birefringence retardation δ'_{PEM} of the PEM ($\delta'_{PEM} = A\sin(\omega t)$), and $J_1(A)$ and $J_2(A)$ are Bessel function coefficients. A was chosen so that the dc component is independent of δ'_{PEM} and χ. This is

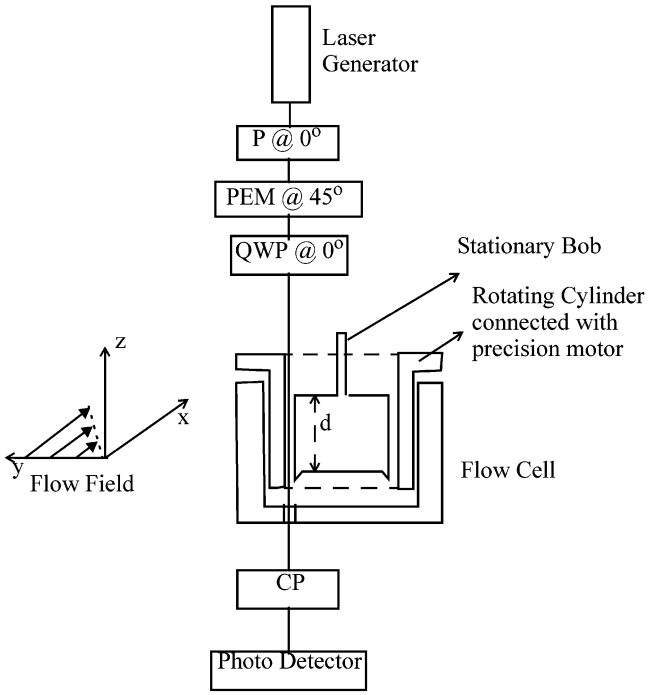

Figure 1. Optical setup and the flow cell fixture used to measure flow birefringence.

achieved when the zero-order Bessel function $J_0(A)$ is zero. (Theoretically, A is 2.401. In this work, A was experimentally found to be around 2.307.) For an anisotropic medium under planar-Couette shear flow, the principal axis of the refractive index tensor deviates from the flow direction with an orientation angle χ. $\delta' = 2\pi\delta\Delta n'/\lambda$ is the birefringence retardation of the sample ($\Delta n' = n_1 - n_2$ is the birefringence difference between two principal values of the refractive index tensor in the flow plane).[18]

The Fourier coefficients $R_1 = -2J_1(A)\cos(2\chi)\sin\delta'$ and $R_2 = -2J_2(A)\sin(2\chi)\sin\delta'$ of the optical intensity were isolated using the lock-in amplifiers tuned to ω and 2ω and a low-pass dc filter. From R_1 and R_2, δ' (hence $\Delta n'$) and χ can be calculated. According to the following relationships

$$n_{xy} = 0.5\Delta n' \sin 2\chi \tag{2}$$

$$n_{xx} - n_{yy} = \Delta n' \cos 2\chi \tag{3}$$

n_{xy}, n_{xx}, and n_{yy} are components of the anisotropic refractive index tensor $\mathbf{\Delta n}$ for a fluid subject to simple shear flow in the $x-y$ plane

$$\mathbf{\Delta n} = \begin{bmatrix} n_{xx} & n_{xy} & 0 \\ n_{xy} & n_{yy} & 0 \\ 0 & 0 & 0 \end{bmatrix} \tag{4}$$

When the refractive index is low, the experimental error becomes large. Therefore, we discarded all refractive index values below 5×10^{-10} where the estimated error is ±20%. If the refractive index is above 10^{-8}, the experimental error is almost negligible (<1%).

For polymer liquids in simple shear flow a simple linear relationship between the stress tensor $\boldsymbol{\tau}$ and $\mathbf{\Delta n}$ is often found.[19] This relationship is called the stress−optical rule

$$\mathbf{\Delta n} = C\boldsymbol{\tau} \tag{5}$$

where C is the stress−optical coefficient. However, it will break down under the following situations.[18,20] First, when polymer chains undergo large-scale extensions, the Gaussian chain assumption no longer holds. Therefore, both $\boldsymbol{\tau}$ and $\mathbf{\Delta n}$ are no longer simply proportional to the second moment tensor $\langle\mathbf{RR}\rangle$ of the end-to-end vector $\mathbf{R}$, resulting in the failure of the stress−optical rule. Second, when a system is not optically uniform, as in the case of polymer blends, or contains mesoscopic structures such as phase domains or secondary colloidal structures, the stress−optical rule fails. For polymer blends, each component contributes differently to stress and birefringence even if they are homogeneously mixed. In the latter case, the anisotropic shape of mesoscopic structures under flow produces a so-called form birefringence, which may have much different stress−optical behavior from primary structures. In addition, the stress−optical rule is only valid on time scales beyond the glass transition, where the dynamics are dominated by entropic contributions.

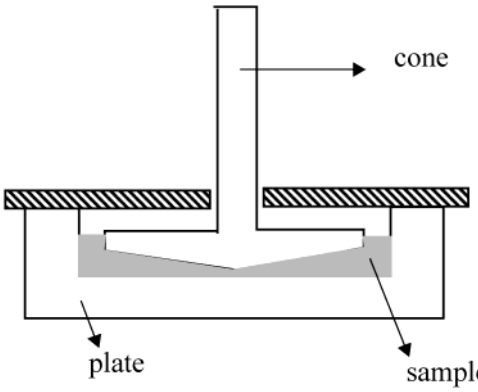

Figure 2. Cone−plate fixture used in mechanical rheology experiment.

Mechanical Rheometry. A Paar Physica MCR300 rheometer with cone and plate fixtures was used to measure flow properties of PEO−silica dispersions. The cone diameter was 50 mm, and the cone angle was 1° for all measurements. Therefore, the cone surface area is large enough to acquire good quality data, even at low polymer concentrations. The temperature was always set to be 25 °C. Because these dispersions have low viscosity, the fixture design shown in Figure 2 was adopted to maintain the sample in the cone−plate gap. Another advantage of this design is that the flow cell can be sealed, minimizing water evaporation during experiments. Steady shear experiments were carried out at constant shear rate $\dot{\gamma}$ and the shear stress $\sigma_{xy}(t)$ during start-up flow, under steady flow, and after cessation of flow recorded.

Dynamic Light Scattering. Diffusive features detected using dynamic light scattering have been known for many years to shed light on structures and dynamics of polymer solutions and colloidal systems.[21,22] In this work, a dynamic light scattering (DLS) apparatus was used to study diffusive behavior of PEO−silica dispersions at room temperature. The light source is a Lexel model 85 argon ion laser with a wavelength λ_d of 488 nm. Light passing through the sample cell was collected with an EMI 9789B photomultiplier tube. The output signal was amplified using an amplifier−discriminator and then sent to a Brookhaven Instruments BI-2030AT correlator. The measured time correlation of scattered light intensity gives characteristic decay times τ_c of different diffusive modes. τ_c is related to the diffusion coefficient D as $D = q^2/\tau_c$. Here, q is the scattering vector defined as $q = 4\pi n \sin(\theta/2)/\lambda_d$ with n the solution refractive index and θ the scattering angle. The viscosities of samples used in DLS measurements were determined using capillary viscometry.

Result and Discussion

When an aqueous PEO−silica dispersion is subjected to flow, anisotropic alignment of PEO chains and deformation of silica particle clusters can both contribute to flow birefringence. Form birefringence of isolated silica particles is small since they are nearly isotropic in shape. Flow birefringence experiments using silica suspensions with particle volume fraction ϕ up to 16 vol % reveal negligible birefringence in Couette shear flow at shear rates in the range of interest for this study.

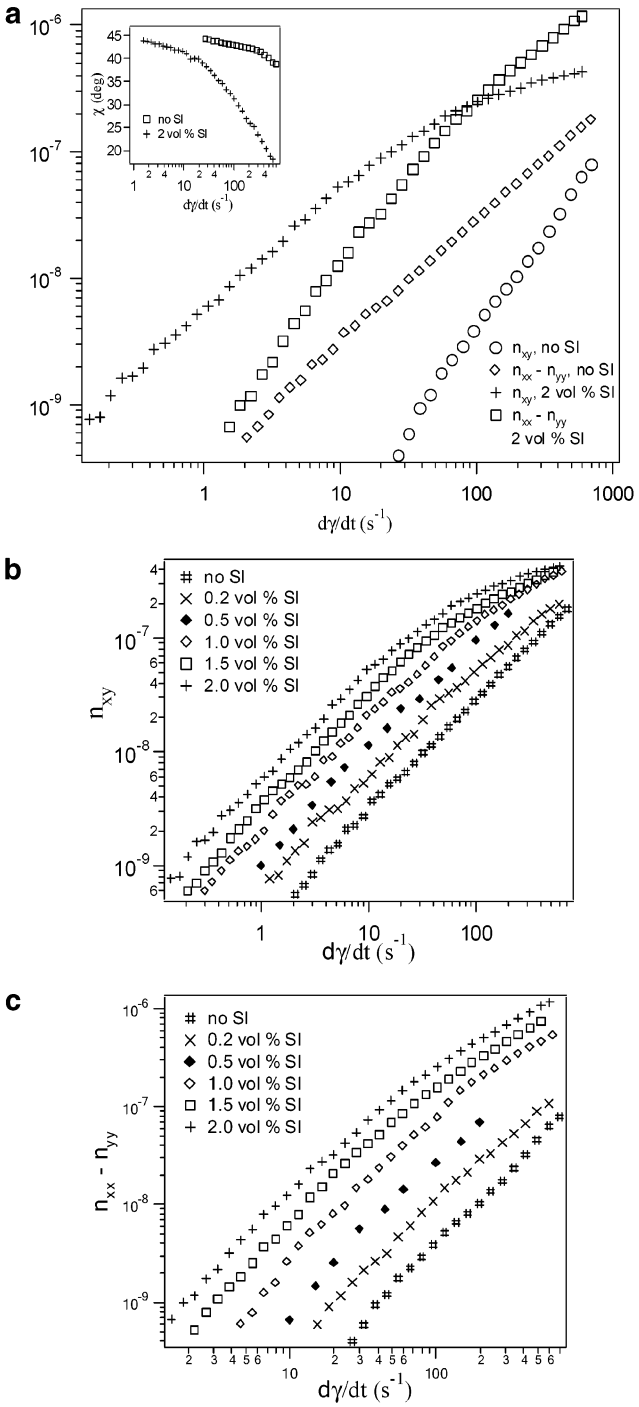

Figure 3. (a) A log−lot plot of birefringence components n_{xy} and $n_{xx} - n_{yy}$ vs shear rate $\dot{\gamma}$ (flow curve) of a pure PEO solution and a PEO−silica dispersion with 2 vol % silica particles. The inset shows the orientation angle χ as a function of $\dot{\gamma}$. (b) A log−log plot of n_{xy} vs $\dot{\gamma}$ of PEO−silica dispersions with various particle volume fractions ϕ. (c) A log−log plot of $n_{xx} - n_{yy}$ vs $\dot{\gamma}$ of PEO−silica dispersions with various ϕ. The polymer concentration is 4.6 wt %, and the molecular weight M_w is 700 000 g/mol.

The volume fraction ϕ of silica in PEO−silica dispersions studied in this work is at most 2 vol %. Therefore, the form contribution of silica particles to the overall flow birefringence of the dispersion is expected to be negligible in comparison to birefringence generated by PEO chains or PEO−silica secondary structures.

The birefringence components n_{xy} and $n_{xx} - n_{yy}$ measured at variable shear rate $\dot{\gamma}$ in steady shear flow

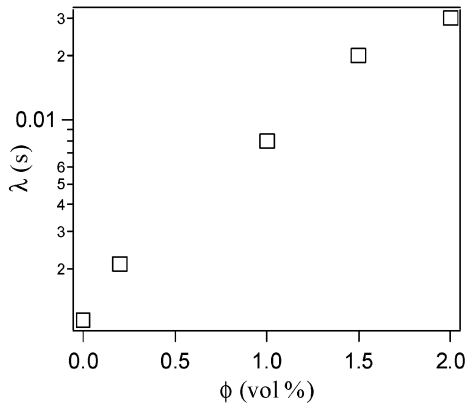

Figure 4. Estimated characteristic relaxation time λ of PEO−silica dispersions as a function of ϕ. The polymer concentration is 4.6 wt %, and the molecular weight M_w is 700 000 g/mol.

are summarized in Figure 3a−c. Data in Figure 3a are for the neat PEO solution and for the same PEO solution containing 2 vol % silica nanospheres. ($\bar{d}$ = 12 nm. In this following text, $\bar{d}$ is by default 12 nm if it is not explicitly stated.) The overlapping concentration c^* for the polymer is estimated to be ∼0.1 wt %,[23] and therefore c is about 46c^*. It is evident from the figure that even at this relatively high solution concentration, addition of nanosized silica particles dramatically increases (by about 1 order of magnitude) both components of the birefringence. In addition, while the neat PEO solution exhibits nearly classical liquidlike birefringence scalings throughout the range of shear rates studied ($n_{xy} \sim \dot{\gamma}^{1\pm0.03}$; $n_{xx} - n_{yy} \sim \dot{\gamma}^{1.65\pm0.05}$), a transition to more complex, shear thinning characteristics is seen for the PEO−silica dispersion. This transition coincides with the appearance of a new flow regime, $\dot{\gamma} > 125\ s^{-1}$, in which $n_{xx} - n_{yy}$ becomes larger than n_{xy}. Physically, such a regime is anticipated when shearing becomes persistent enough to orient and stretch the fundamental fluid elements (e.g., polymer molecules) at a rate faster than thermal forces randomize such orientation (i.e., $Wi \equiv \lambda\dot{\gamma} > 1$, where Wi is the Weissenberg number and λ the characteristic terminal relaxation time of the fluid). The scaling exponent 1.65 found experimentally for $(n_{xx} - n_{yy})(\dot{\gamma})$ is smaller than the theoretical value 2 for entangled polymer solutions.[24] The orientation angle $\chi \equiv {}^1/_2\ \mathrm{atan}[2n_{xy}/(n_{xx} - n_{yy})]$ (inset of Figure 3a) is also seen to decrease much more quickly with increasing shear rate for the PEO−silica dispersion than for the PEO solution, which is consistent with the idea that fluid elements relax more slowly in the dispersions.

Figure 3b,c shows the effect of silica particle volume fraction on $n_{xy}(\dot{\gamma})$ and $(n_{xx} - n_{yy})(\dot{\gamma})$. It is apparent from this figure that the behavior observed in Figure 3a is part of a continuum. Specifically, it is seen that as the particle volume fraction is increased, the $n_{xy}(\dot{\gamma})$ and $(n_{xx} - n_{yy})(\dot{\gamma})$ curves progressively shift to the left, indicating that the criterion $Wi > 1$ is reached at progressively lower shear rates. This means that the average relaxation time λ of the dispersions is larger than that of the neat PEO solution for particle volume fractions as low as 0.2%. This effect is quantified in Figure 4, which shows that the effective characteristic relaxation time of the fluid increases by more than an order of magnitude when the particle volume fraction is varied from 0 to 2%. Here we define the effective characteristic relaxation time using Zimm theory[3]

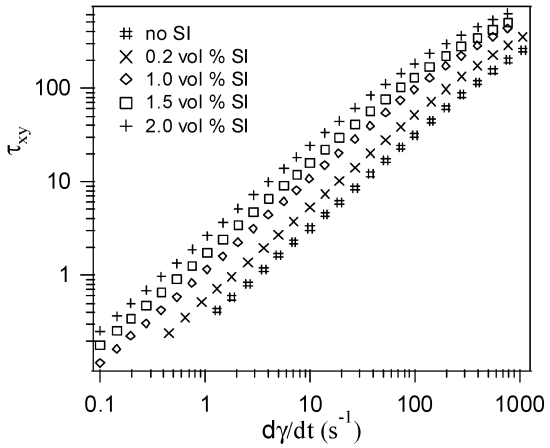

Figure 5. Shear rate $\dot{\gamma}$ dependent shear stress τ_{xy} of PEO−silica dispersions with different ϕ. The polymer concentration is 4.6 wt %, and the molecular weight M_w is 700 000 g/mol.

$$\lambda = \frac{1}{2}\lim_{\dot{\gamma}\to 0}\frac{\psi_1}{\eta} \tag{6}$$

Here, $\psi_1 \equiv (\tau_{xx} - \tau_{yy})/\dot{\gamma}^2$ is the first normal stress coefficient ($\tau_{xx} - \tau_{yy}$ is the first normal stress difference) and $\eta \equiv \tau_{xy}/\dot{\gamma}$ is the shear viscosity. If the stress−optical rule holds in the low shear rate limit (this condition will be proven valid in the following discussions of stress−optical behavior), eq 6 can be rewritten in terms of quantities measured from our birefringence experiments

$$\lambda = \frac{1}{2}\lim_{\dot{\gamma}\to 0}\frac{\tau_{xx} - \tau_{yy}}{\dot{\gamma}\tau_{xy}} = \lim_{\dot{\gamma}\to 0}\frac{n_{xx} - n_{yy}}{2\dot{\gamma}n_{xy}} \tag{7}$$

Measurements of τ_{xy} under steady shear flow were performed independently using the same PEO−silica dispersions. $\tau_{xy}(\dot{\gamma})$ for these materials are shown in Figure 5. These results clearly mimic those in Figure 3b quite well, particularly at low shear rate. Thus, slower relaxation of fluid elements in the dispersions also enhances their flow viscosity η. Whenever the stress−optical rule holds, $n_{xy}/\dot{\gamma}$ will be proportional to η. Therefore, $n_{xy}/\dot{\gamma}$ can be regarded as the optical analogue of shear viscosity. Figure 6a,b shows the shear rate dependent $n_{xy}/\dot{\gamma}$ and η of these dispersions. Although the pure PEO solution exhibits shear rate independent $n_{xy}/\dot{\gamma}$ and η throughout the experimental shear rate window, all dispersions containing nanoparticles show a zero-shear plateau of $n_{xy0}/\dot{\gamma}$ and η_0 followed by a shear thinning zone. Using the method described above to estimate the characteristic relaxation time λ, we can rescale the axes of Figure 6a,b and plot n_{xy}/n_{xy0} and η/η_0 as functions of the Wiessenberg number Wi in Figure 6c,d. Although the overlap is imperfect, the data do appear to be describable in terms of a master curve, suggesting that fundamental fluid elements in PEO−silica dispersions with different ϕ follow similar relaxation dynamics. This finding also clearly shows that the earlier onset of shear thinning seen in dispersions with higher ϕ is a consequence of the longer relaxation time λ.

More careful scrutiny of Figure 6a,b reveals important new information about PEO−silica dispersions. It is for example evident from these figures that despite the visual similarity of η and $n_{xy}/\dot{\gamma}$, η is less shear thinning than $n_{xy}/\dot{\gamma}$. This means that the stress−optical rule is likely violated in these materials. Also, at high shear

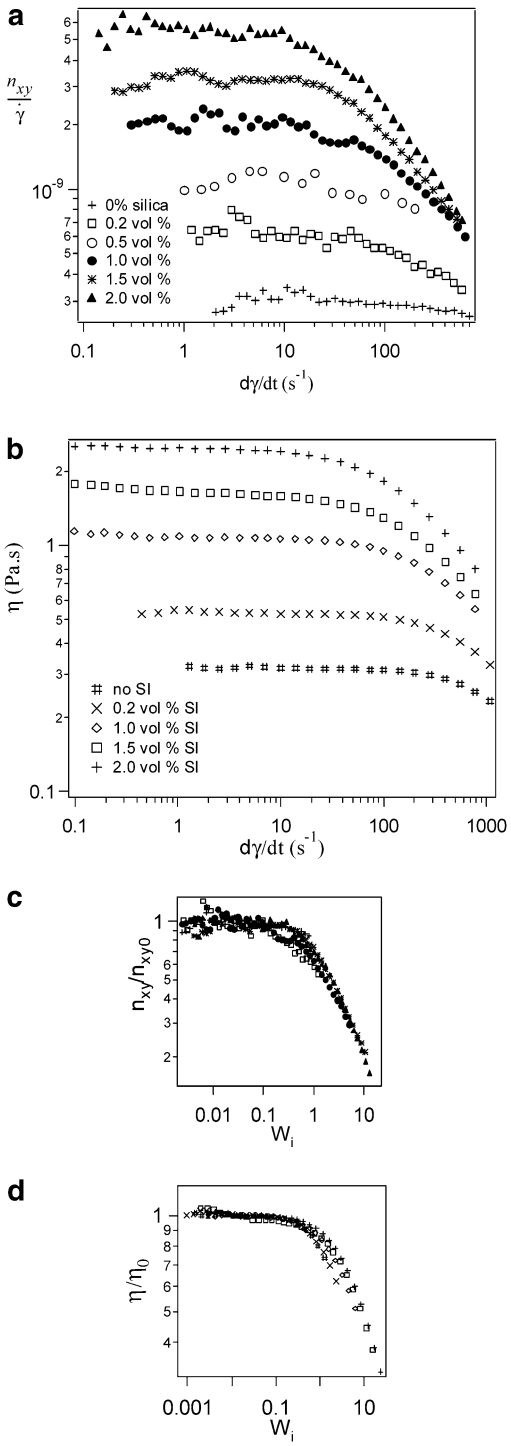

Figure 6. (a) Shear rate $\dot{\gamma}$ dependent $n_{xy}/\dot{\gamma}$ of PEO−silica dispersions with various particle volume fractions ϕ. (b) Shear viscosity η as a function of $\dot{\gamma}$. (c) Comparison of flow curves examined in (a) under normalized scales. (d) Comparison of flow curves examined in (b) under normalized scales. The polymer concentration is 4.6 wt %, and the molecular weight M_w is 700 000 g/mol.

rates, the $n_{xy}/\dot{\gamma}$, and to a lesser degree $\eta(\dot{\gamma})$, plots at variable ϕ appear to converge. Such convergence is possible if the fundamental flow elements responsible for the birefringence break down and become comparable in size at high shear rates or, alternatively, if the shear stress in the dispersions saturate at a ϕ-independent value at high rates. The latter possibility has been discussed in the case of PEO−silica nanocomposite melts,[6] where the high-frequency moduli were found to

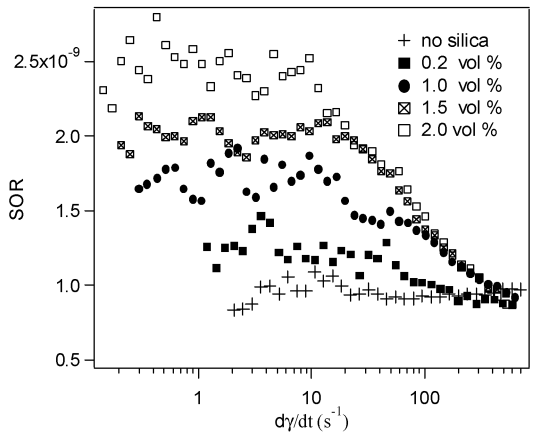

Figure 7. Stress−optical ratio (SOR) as a function of $\dot{\gamma}$ of PEO−silica dispersions with different ϕ. The polymer concentration is 4.6 wt %, and the molecular weight M_w is 700 000 g/mol.

be insensitive to ϕ compared with low-frequency responses. However, $n_{xy}(\dot{\gamma})$ and $\tau_{xy}(\dot{\gamma})$ shown in Figures 3b and 4 are far from ϕ-independent even at the highest shear rate. Therefore, the second possibility seems not the case here. To explore the first possibility further, we consider the stress−optical behavior of the dispersions.

The stress−optical rule relates the stress tensor and the refractive index tensor linearly with a stress−optical coefficient C independent of shear rate. For any fluid, whether or not it obeys this rule, a stress−optical ratio (SOR) can be defined in the following way to describe its stress−optical behavior

$$\mathrm{SOR} \equiv \frac{n_{xy}}{\tau_{xy}} \tag{8}$$

When the stress−optical rule is valid, SOR is obviously equal to C. Unlike homopolymer solutions, fluids containing mesoscopic microstructures usually exhibit complex stress−optical behavior.[10,20] Plots shown in Figure 7 are fully supportive of this point. The neat polymer solution obeys the stress−optical rule throughout the shear rate range. The stress−optical coefficient C (or SOR) is around 0.9×10^{-9} Pa^{-1}. We have not found a reported C value of linear PEO aqueous solution in the literature yet. C of the PEO network swollen in water[25] and of PEO melts[26] were found to be close to that of linear PEO aqueous solution measured in this study. SOR of dispersions containing nanoparticles has a weak dependence upon $\dot{\gamma}$ when $\dot{\gamma}$ is small and decreases at high $\dot{\gamma}$. Comparing Figure 7 with Figure 6, it can be seen that the plateaulike regime of SOR coincides with the linear flow regime ($Wi < 1$). The plateau value of SOR is denoted as SOR_0 and shown in Figure 8. Clearly, SOR_0 is an increasing function of ϕ. When the flow is no longer linear, the stress−optical rule breaks down. An interesting finding here is that SOR of all the dispersions approaches the stress−optical coefficient of the neat polymer solution at very high shear rate. This behavior indicates that dispersions with different ϕ regain similar stress−optical behavior under strong shear flows, which would be consistent with flow-induced breakdown of fundamental flow units above a well-defined flow rate.

The specific viscosity $\eta_s(\phi) = \eta_0(\phi)/\eta_0(0)$ can be obtained by averaging viscosity data in the plateau regime

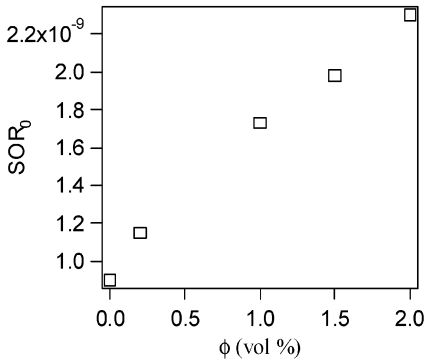

Figure 8. Zero-shear stress−optical ratio (SOR_0) of PEO−silica dispersions examined in Figure 7 vs ϕ.

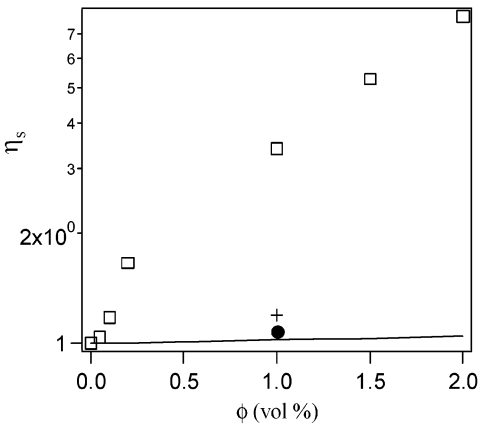

Figure 9. A log−linear plot of zero-shear viscosity η_s vs ϕ. (The solid line represents the prediction of the Einstein equation: □, dispersions filled with 12 nm bare silica particles; ●, dispersions filled with surfaced modified 12 nm silica particles; +, dispersion filled with 0.1 μm bare silica particles.) The polymer concentration is 4.6 wt %, and the molecular weight M_w is 700 000 g/mol.

exhibited in Figure 6b. Figure 9 shows two distinct regimes with the critical particle volume fraction $\phi_c \sim 0.2\%$. At $\phi > \phi_c$, η_s has a weaker dependence on ϕ. The solid line in Figure 9 is the suspension viscosity predicted by the Einstein equation assuming the polymeric medium is a simple viscous liquid

$$\eta_s(\phi) = 1 + 2.5\phi \tag{9}$$

There is clearly a large difference between the experimental data and the Einstein equation prediction. For example, the Einstein equation gives a 5% viscosity increase at $\phi = 2\%$. However, the dispersion with 2 vol % nanoparticles shows a zero-shear viscosity 750% as high as that of the pure PEO solution, suggesting that PEO−silica dispersions behave far from colliding hard spheres in a continuum medium.

All the unusual flow behavior of PEO−silica dispersions described above, we believe, is due to dynamics of secondary structures. Fundamental fluid elements are now polymer−particle clusters. On one hand, they relax more slowly than individual polymer chains, resulting in longer characteristic relaxation time of the dispersion; on the other hand, they enhance the dynamic viscosity and the optical anisotropy under flow. Since PEO chains have strong affinity to silica particles, thermal energy is too weak to break the polymer bridges in our experimental time scales. At low shear rates, these soft secondary structures do not break and are linearly

deformed, resulting in Newtonian flow profile. At $Wi > 1$, they are strongly deformed and ruptured (the polymer bridges are broken under strong shear fields), causing shear thinning. Repeatability of the experimental results indicates that their equilibrium state will be recovered after cessation of flow.

In the frame of secondary structure dynamics, the mechanism of the observed complex stress−optical behavior can be described as follows. The increase of SOR_0 by adding more nanoparticles in the dispersion is probably due to the form birefringence effect. Loose secondary polymer−particle structures can be easily deformed and oriented by flow. They become optically anisotropic, resulting in form birefringence. These structures do not contribute as much to the stress as individual polymer chains, leading to enhanced SOR_0. As the particle loading increases, the form effect becomes more prominent and SOR_0 increases. When W_i is small, these secondary structures deform linearly, and the measured SOR has a very weak dependence upon $\dot{\gamma}$. At $W_i > 1$, they start to break up since they cannot fully relax within the characteristic flow time $1/\dot{\gamma}$. The force applied on them is strong enough to cause rupturing of polymer−particle bridging connections. Consequentially, reduction of the size and number of secondary structures lowers the form contribution and therefore lowers the SOR. Under very strong shear flow ($W_i \gg 1$), most of the secondary structures are destroyed, and the form contribution becomes negligible. The stress−optical behavior is then dominated by dynamics of polymer chains alone. Therefore, SOR of polymer−particle dispersions will be equal to that of the pure polymer solution at $W_i \gg 1$. The dispersion with 0.2 vol % particles shows a second plateaulike regime at very high shear rates (Figure 7) with data points almost overlapping with those of the pure polymer solution. For samples with $\phi > 0.2\%$, their SOR just approaches that of the pure polymer solution at the highest experimental shear rate, though overlapping of SOR is expected at even higher shear rate.

Figure 9 shows a weaker ϕ dependence of zero-shear viscosity at $\phi > \phi_c$. A hard-sphere suspension usually exhibits a stronger dependence of η_s upon ϕ as ϕ increases,[3] which differs from the phenomenon observed here. Hard-sphere suspensions contain nondraining particles, while fundamental fluid elements of PEO−silica dispersions are far from the nondraining limit. The existence of a critical particle volume fraction ϕ_c is probably because polymer−particle clusters strongly interpenetrate each other when ϕ reaches ϕ_c. A similar phenomenon was observed in our previous study of PEO−silica nanocomposite melts,[6] in which we found that when ϕ is over 2.0%, a percolated polymer−particle network forms, and the dependence of viscoelastic properties such as moduli on ϕ becomes much weaker.

Finally, the dramatic increase of zero-shear viscosity η_0 with increasing ϕ manifests a strong interaction between particles. This interaction can originate from the polymer bridging interaction or the van der Waals attraction or both. Our previous study on PEO−silica nanocomposites[6] in the melt state concluded that polymer−particle interactions are the most important determinant of rheological property enhancement when particle size becomes comparable to polymer random coil size. Consider PEO−silica dispersions with polymer molecular weight $M_w = 700\,000$ g/mol. The radius of gyration R_g in a aqueous solution was found to be around 50 nm.[23] The average polymer random coil diameter can be estimated to be $2R_g = 100$ nm. Therefore, in our model systems, particle size is much smaller than polymer random coil size. This will result in a high bridging density even at a modest particle loading since individual polymer chains can link multiple particles. This condition plus strong adsorption strength (hydrogen bonding) leads to a strong polymer−particle bridging interaction, and we expect that this interaction plays the most important role in dynamics of PEO−silica dispersions.

Table 1. Zero-Shear Viscosity and Birefringence

particle volume fraction (vol %)	polymer concn (wt %)	polymer mol wt (g/mol)	η_0 (Pa s)	$(n_{xy}/\dot{\gamma})\|_{\dot{\gamma}\to 0}$ (s)
$\phi = 1.5$	4.6	700 000	1.68	3.20×10^{-9}
$\phi = 1.5$	4.6	178 000	0.12	3.98×10^{10}
$\phi = 1$	4.6	700 000	1.08	1.96×10^{-9}
$\phi = 1$	2.3	700 000	0.11	5.19×10^{10}
$\phi = 0$[a]	4.6	700 000	0.33	3.01×10^{10}
	4.6	178 000	0.038	3.83×10^{-11}
	2.3	700 000	0.039	3.99×10^{-11}

[a] Pure polymer solution.

To support the arguments above, several additional experimental tests were carried out. First, we studied the flow behavior of a PEO−silica dispersion with surface-modified particles. Its specific viscosity η_s is shown in Figure 9. It is obvious from Figure 9 that surface modification largely reduces the zero-shear viscosity, which is now only slightly above the line depicted by the Einstein equation. When the surface is coated with o-PEO silanes, adsorption of silanol groups is so strong that it becomes difficult for long PEO chains in the solution to adsorb to the surface. Hence, the bridging effect is largely reduced. This experiment confirms that the bridging interaction, rather than direct particle−particle interactions, is mainly responsible for the enhanced viscosity and flow birefringence of PEO−silica dispersions.

A dispersion with submicron size silica particles ($\bar{d} = 0.1\,\mu$m) was also tested. Its specific viscosity η_s (Figure 9) is very close to the line predicted by the Einstein equation, manifesting that the dispersion containing submicron size particles behaves almost like a simple suspension of hard spheres in a continuum medium. In other words, submicron size particles give almost no rise to the shear viscosity. This result proves that nanoscale interactions are essential for substantial enhancement of rheological properties at low particle volume fractions. It is also consistent with the point that the polymer−particle bridging interaction gets stronger as the particle size get smaller.

The effect of polymer concentration and molecular weight was also explored. We compared PEO−silica dispersions of different polymer concentrations and molecular weights with their pure polymer solution counterparts. All the dispersions were found to have the typical change in flow behavior: enhancement of viscosity and flow birefringence, a longer relaxation time, shear thinning at high shear rate, etc. However, absolute values of shear viscosity and flow birefringence of these dispersions are markedly influenced by polymer concentration and molecular weight (see Table 1). The physics behind this observation is, although percolated PEO−silica structures exist despite different polymer concentrations and molecular weights, polymer concen-

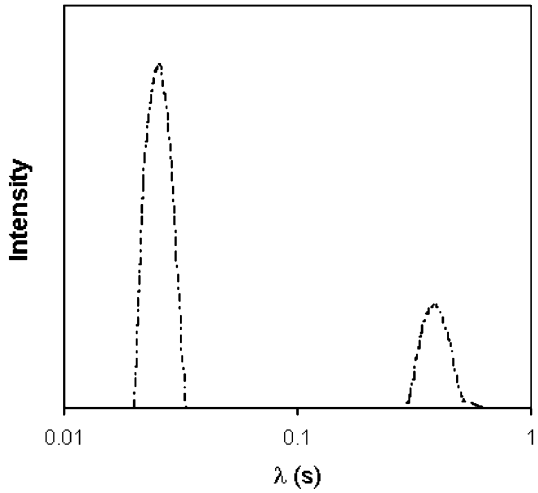

Figure 10. Distribution of relaxation times λ. The sample is a PEO−silica dispersion with polymer concentration at 0.75 wt % and molecular weight M_w at 700 000 g/mol and particle volume fraction $\phi = 0.17\%$.

Table 2. Diffusive Properties of the "Cluster" Mode[a]

polymer concn (wt %)	polymer concn (vol %)	diffusion coeff (m^2/s)	dynamic viscosity (Pa s)
0.75	0	4.8×10^{-13}	$(5.2 \pm 0.1) \times 10^{-3}$
0.75	0.17	5.6×10^{-13}	$(5.1 \pm 0.1) \times 10^{-3}$
0.75	0.25	8.2×10^{-13}	$(5.5 \pm 0.1) \times 10^{-3}$
0.75	0.33	1.0×10^{-12}	$(5.7 \pm 0.1) \times 10^{-3}$
1.15	0.5	3.2×10^{-13}	$(1.2 \pm 0.1) \times 10^{-2}$
2.3	1.0	8.4×10^{-14}	$(3.9 \pm 0.1) \times 10^{-2}$

[a] Polymer molecular weight M_w in all dispersions shown in this table is 700 000 g/mol.

tration and molecular weight strongly influence the density and strength of polymer−particle bridges.

In addition, dynamic light scattering of PEO−silica dispersions at lower concentrations were studied. Usually for semidilute polymeric solutions, several dynamics can be detected: a gellike cooperative mode, a Rouse mode, and a "cluster" mode (from fast to slow). For well-entangled polymer solutions, an additional reptation mode was also reported.[21] Polymer concentration c of our model dispersions used for rheological testing is too high to yield good light scattering results. These dispersions were then diluted to concentrations ranging from c^* to $20c^*$ for DLS study. All DLS measurements show two distinct modes, one fast and one very slow. (An example of the relaxation time distribution is shown in Figure 10.) Characteristic relaxation times λ of these modes are summarized in Table 2. The fast mode has an intensity much higher than the slow one, revealing that it is the cooperative diffusion mode. (In this case, the Rouse mode may be shadowed by this dominant mode.) Since these dispersions are barely in the semidilute regime, the reptation mode should be insignificant. Thus, the slow mode is most probably controlled by diffusive motions of polymer−particle or polymer clusters. (Since PEO tends to aggregate in low concentration solutions, the "cluster" mode of pure PEO solutions is also expected.[27]) The dynamic viscosity η_0 of DLS samples was also measured and shown in Table 2. η_0's of dispersions with fixed c at 0.75 wt % and different particle volume fractions were found to differ from each other only slightly. This seems contradictory to the result shown in Figure 9. In the case of $c = 4.6$ wt %, a particle volume fraction as low as 0.1% will cause substantial increase of viscosity. We think the weak dependence of viscosity on ϕ at $c = 0.75$ wt % is because the bridging density is very low at this polymer concentration. Therefore, the polymer−particle bridging interaction is too weak to noticeably enhance the viscosity. Meanwhile, the characteristic diffusion coefficient D of the "cluster" mode goes up as ϕ increases, suggesting an accelerated concentration fluctuation of polymer−particle clusters. Now the question is, what causes the increase of D with increasing ϕ. As we know, diffusive motion of polymer molecules is between nondraining and free draining limits, while silica beads diffuse in a nondraining manner. Plus, the coil size of polymer chains used in this study is much larger than the particle size. Therefore, diffusion of polymer chains is much slower than that of silica particles. Adding more mobile nanoparticles into a polymer cluster can speed up its local diffusive motion, given that the fluid viscosity is insensitive to the introduction of nanoparticles.

In the second series, a dispersion with 2.3 wt % polymers and 1.0 vol % particles was diluted by 66% (0.75 wt % and 0.33 vol %) and 50% (1.15 wt % and 0.5 vol %), respectively. Viscometry and light scattering results of the two diluted samples plus the nondiluted one are compared (Table 2). The viscosity of the dispersion increases, but the diffusion coefficient of the "cluster" mode decreases with increasing polymer and particle concentrations. When polymer and particle concentrations increase, the number and size of PEO−silica clusters increase and the bridging interaction is strengthened. Thus, a percolated polymer−particle network is progressively developed. As a result, the viscosity is enhanced, and the diffusive concentration fluctuation of polymer-particle clusters is restricted.

Conclusion

Flow properties of PEO−silica aqueous dispersions were studied using mechanical and optical rheometry. Silica particles are much smaller than polymer coils, producing strong polymer bridging interactions even at very low particle volume fraction ϕ. Optical birefringence, shear stress, and shear viscosity were found to increase as ϕ increases. Although the pure polymer solution shows terminal flow behavior throughout the shear rate range, dispersions with nanoparticles exhibit a linear regime followed by a shear thinning regime above a critical shear rate. These properties, we believe, are related to dynamics and flow-induced structural changes of secondary polymer−particle structures. With their size much larger than individual polymer chains, these clusters increase the material viscosity and optical anisotropy. Under strong shear flows, they begin to break down, resulting in shear thinning. As ϕ increases, characteristic relaxation times of the dispersions become larger, and their flow curves are shifted to lower shear rates. The fact that these flow curves can be normalized into a master curve suggests that polymer−particle clusters in these dispersions follow similar relaxation dynamics. The dependence of zero-shear viscosity upon ϕ is dramatically stronger than Einstein equation predicts, confirming that the polymer−particle bridging effect is very strong.

The stress−optical behavior of PEO−silica dispersions is also quite different from that of pure PEO solutions, which obey the stress−optical rule throughout the experimental shear rate window. SOR of polymer−particle dispersions has almost no dependence on shear

rate when it is low and begins to decrease at $W_i > 1$. The plateau value of SOR increases with increasing particle volume fraction. This is because polymer−particle clusters can be easily deformed anisotropically along with the flow direction and contribute to form birefringence that enhances SOR at not too high shear rates. When W_i is larger than unity, they start to be destroyed by the flow. At very high shear rate, the form contribution from secondary structures becomes negligible, and the stress−optical behavior follows that of the pure polymer solution. Therefore, SORs of polymer−particle dispersions approach that of the pure polymer solution.

Dynamic light scattering of dispersions at polymer concentrations above c^* indicates a fast cooperative diffusion mode of polymer chains and a much slower "cluster" mode. When we compare the cluster mode of dispersions with the pure polymer solution with the same polymer concentration ($c \sim 6c^*$), it was found that the concentration fluctuation of polymer−particle clusters is actually faster than that of pure polymer clusters. In this case, nanoparticles diffuse much faster than long polymer chains. Therefore, the diffusive motion of clusters containing nanoparticles is accelerated.

Acknowledgment. We are grateful to the Cornell Center for Materials Research (CCMR), a Materials Research Science and Engineering Center of the National Science Foundation (DMR-0079992), and the National Science Foundation Surfaces program (CMS-0004525) for supporting this study. Very helpful discussions with Professors Claude Cohen and Don Koch are also gratefully acknowledged.

References and Notes

(1) Messersmith, P. B.; Stupp, S. I. *J. Mater. Res.* **1992**, *7*, 2599.
(2) Huang, X. Y.; Brittain, W. J. *Macromolecules* **2001**, *34*, 3255.
(3) Larson, R. G. *The Structure and Rheology of Complex Fluids*, Oxford: New York, 1999.
(4) Pham, Q. T.; Russel, W. B.; Thibeault, J. C.; Lau, W. *J. Rheol.* **1999**, *43*, 1599.
(5) Horigome, M.; Otsubo, Y. *Langmuir* **2002**, *18*, 1968.
(6) Zhang, Q.; Archer, L. A. *Langmuir* **2002**, *18*, 10435
(7) Krishnamoorti, R.; Giannelis, E. P. *Macromolecules* **1997**, *30*, 4097.
(8) Schmidt, D.; Shah, D.; Giannelis, E. P. *Curr. Opin. Solid State Mater. Sci.* **2002**, *6*, 205.
(9) Iler, R. K. *J. Colloid Interface Sci.* **1971**, *37*, 364.
(10) Schmidt, G.; Nakatani, A. I.; Han, C. C. *Rheol. Acta* **2002**, *41*, 45.
(11) Rubio, J.; Kitchener, J. A. *J. Colloid Interface Sci.* **1976**, *57*, 132.
(12) Russel, W. B.; Saville, D. A.; Schowalter, W. R. *Colloidal Dispersions*; Cambridge University Press: Cambridge, 1989.
(13) de Gennes, P. G. *Macromolecules* **1982**, *15*, 492.
(14) Scheutjens, J. M. H. M.; Fleer, G. J. *Macromolecules* **1985**, *18*, 1882.
(15) Kapsabelis, S.; Prestidge, C. A. *J. Colloid Interface Sci.* **2000**, *228*, 297.
(16) Jimenez, J.; de Joannis, J.; Bitsanis, I.; Rajagopalan, R. *Macromolecules* **2000**, *33*, 8512.
(17) Chen, S. P.; Archer, L. A. *J. Polym. Sci., Polym. Phys.* **1999**, *37*, 825.
(18) Fuller, G. G. *Optical Rheometry of Complex Fluids*; Oxford University Press: New York, 1995.
(19) Janeschitz-Kriegl, H. *Polymer Melt Rheology and Flow Birefringence*; Springer-Verlag: New York, 1983.
(20) Kannan, R. M.; Kornfield, J. A. *J. Rheol.* **1994**, *38*, 1127.
(21) Stepanek, P.; Brown, W. *Macromolecules* **1998**, *31*, 1889.
(22) Sedlak, M.; Amis, E. J. *J. Chem. Phys.* **1992**, *96*, 817.
(23) Devanand, K.; Selser, J. C. *Macromolecules* **1991**, *24*, 5943.
(24) Doi, M.; Edwards, S. F. *The Theory of Polymer Dynamics*; Clarendon: Oxford, 1986.
(25) Ishikawa, T. *Polym. J.* **1973**, *5*, 227.
(26) Champion, J. V.; Dandridge, A. *Polymer* **1978**, *19*, 632.
(27) Hand, J. H.; Williams, M. C. *Chem. Eng. Sci.* **1973**, *28*, 63.

MA035667V